Bodur *et al. Discover Concrete and Cement* (2025) 1:21
https://doi.org/10.1007/s44416-025-00019-3

Discover Concrete and Cement

RESEARCH Open Access

Production of high-performance cementless foam composites: gypsum-based and hemp fibre reinforced green systems

Burak Bodur[1], Oğuzhan Yavuz Bayraktar[2] and Gökhan Kaplan[3*]

*Correspondence:
Gökhan Kaplan
gkaplan@atauni.edu.tr
[1]Project and Technology Office, Bartın University, Bartın 74100, Turkey
[2]Department of Civil Engineering, Kastamonu University, Kastamonu 37100, Turkey
[3]Department of Civil Engineering, Atatürk University, Erzurum 25230, Turkey

Abstract
This study investigated the physical, mechanical, durability and microstructural properties of gypsum-based foam composite reinforced with hemp fiber (HF). A gypsum-based foam composite was produced using foam contents of 20, 50, and 80 kg/m^3, and hemp fiber (HF) concentrations of 0%, 1%, and 2%. Additionally, pumice aggregates in the range of 0–4 mm were used in the mixture to support the lightweight foam concrete employed in the study. The demolded specimens were stored at a temperature of 30 °C and a relative humidity of 65%. The flow diameters of the mixtures, which indicate the workability of the mixtures from the fresh state properties, vary between 212 and 288 mm. Fresh unit weights vary between 862 and 1269 kg/m^3, while dry unit weights vary between 723 and 1203 kg/m^3. The mixtures' apparent porosity and water absorption values increased as the foam volume increased; the highest apparent porosity was 57.8%, and the highest water absorption value was 96.14% at a foam volume of 80 kg/m^3. In terms of mechanical properties, the strength decreased as the foam volume increased. The highest compressive strength of 3.93 MPa was obtained with a foam volume of 20 kg/m^3 and 1% HF, while the highest flexural strength of 0.43 MPa was obtained with the same foam volume and 2% HF. The highest compressive strength of 1.34 MPa was achieved even at a foam volume of 80 kg/m^3, which exhibited the lowest mechanical properties. In addition, to determine the durability properties of the blends, they were exposed to high temperatures of 250, 500, and 750℃, and weight losses, UPV changes, and mechanical property changes were investigated. After 750℃ high temperature, mixtures with 20 kg/m^3 foam content showed the highest mechanical properties, while mixtures with 80 kg/m^3 foam content showed a compressive strength of 0.32 MPa. The depths of capillary water treatment of the studied mixtures varied between 14.79 and 19.17 kg/m^2. As a result, this study determined that gypsum can be used as a binder in non-bearing foam concrete, with a foam content of 20 kg/m^3 and a 1% HF addition.

Keywords Foam composite, Gypsum composites, Hemp fiber, Pumice, Sustainability

1 Introduction

The rise in living standards and economic development has led to the growth of the construction sector. With the development of the building sector, cement-based materials are the world's most widely used building materials for the production of structural and non-carrier building elements [1]. The significant advantages of this binder have always made it a preferred choice in mortar and concrete production. With the increasing environmental changes resulting from the greenhouse effect, the environmental impacts of cement production must be seriously considered. Cement is produced at a very high temperature of about 1450℃. It involves an energy-intensive production process and consumes enormous amounts of exhaustible natural resources and fossil energies. In 2017, cement production was responsible for approximately 8% to 9% of global CO_2 emissions, one of the leading greenhouse gases and a significant contributor to global warming. Since 2018, the global annual production of ordinary Portland cement has exceeded 4.1 billion tons and continues to grow. For all these reasons, it is necessary to use alternative binders that have less environmental impact and can reduce cement consumption [2, 3]. Part of the structural elements is provided by foam concrete, classified by unit weight. Foam concrete, which has become prominent especially among lightweight building materials, is recognized as the most common due to its porous structure [4]. Foam concretes are generally used in bridge and road constructions, subway tunnels and exterior wall insulation to reduce the structure's weight. In contrast, its use has been limited in some applications requiring relatively high strength [5]. X. Cong et al. [6] investigated the effect of different fiber reinforcements in foam concrete. In line with this study, it is understood that adding fiber to foam concrete increases the compressive and flexural strengths. It was observed that fibers pierced air bubbles during the preparation of foam concrete; thus, the addition of fibers to fresh foam concrete affected its workability and rheological properties.

Lower density, higher strength-to-weight ratio, lower thermal conductivity coefficients, improved fire resistance, enhanced durability properties, and better sound insulation are characteristics of foam concrete. Amran et al. [7] reported that foam concrete with a density of 1600 kg/m^3 has a thermal conductivity of up to 0.66 W/mK, and foam concrete with a density of 2200 kg/m^3 has a thermal conductivity of up to 1.6 W/mK. The thermal insulation of foam concrete depends on the foam content rather than the binding material content. Materials with significantly lower thermal conductivity often exhibit low strength due to numerous and substantial air gaps [8]. The fact that foam concrete is used as an insulation material due to its structure, which features millions of independent cavities, and its low thermal conductivity, which makes it more resistant to fire, is what sets it apart and makes it a preferred choice over traditional concrete.

At this point, the gypsum material, which is generally used for heat and sound insulation and provides fire resistance when used as a binder in foam concrete production, is evaluated in terms of its advantages and disadvantages. Gypsum stands out as a more environmentally friendly material than cement. Gypsum is one of the oldest building materials in the world, with its application dating back to approximately 7000 BC [9]. The advantages of gypsum material include its high-temperature resistance, good heat and sound insulation, low energy consumption, low cost, environmental friendliness, and recyclability through an appropriate process. However, its sensitivity to water and moisture, as well as its fragile structure, are shown as disadvantages [10]. The fire resistance of gypsum is based on its low thermal conductivity and high endothermic dehydration process [11]. These properties of gypsum have proven to be effective in retarding the temperature rise in a fire environment [12]. In addition, to overcome the disadvantage of low water resistance, the strength of the gypsum matrix is enhanced by adding mineral additives such as fly ash and slag, thereby strengthening its brittle structure [13–15]. At the same time, as the fire resistance requirements of buildings are receiving intense attention, it is becoming increasingly important for safety and industrial purposes to evaluate fire behavior and gain detailed knowledge about gypsum materials exposed to high temperatures. Studies on the fire resistance properties of gypsum-based materials have focused on pure gypsum and commercial foamed gypsum board, the most widely used gypsum products today. For example, Thomas et al. [12] reviewed the relevant literature and chemistry of the dehydration reactions that gypsum undergoes when heated. Ghazi et al. and Park et al. [16, 17] investigated the thermal behavior of a standard gypsum board in the event of a fire. Rahmanian et al. [18] proposed a combined numerical and experimental method to extract the thermal conductivity of various gypsum board products at elevated temperatures. However, there are almost no studies on combining gypsum with foam concrete to support its lightness and fire resistance and reinforce the resulting composite with organic fibers.

Fibers are also added to gypsum to obtain a fiber-gypsum matrix composition. The development of cracks, when subjected to tensile stress, can be prevented by the bridging effect between the fibers or matrix. The flexural strength and toughness of the gypsum matrix help to improve it effectively. When the literature is examined, organic or vegetable fibers, such as straw and coconut, and inorganic fibers, such as glass and carbon fiber, are used to reinforce the gypsum matrix [19]. Among natural fibers, hemp fibers (HF) are the most widespread due to their use in biofuels, textiles, food, automotive and construction [20]. These fibers have found applications in the construction industry, including lime-hemp plaster, insulation, hemp concrete, and polymeric hemp-based composites [21–23]. Çomak et al. [24] investigated the strengths, unit weights, water absorption and flexural strengths of HF in different ratios and lengths. This study achieved the optimum result with a 12 mm length and a 2–3% HF concentration. Hamzaoui et al. [25] used 3% HF to minimize the adverse effect on mechanical strength. Ruano et al. [26] investigated the flexural behavior of cement-based composites incorporating HF and sugarcane bagasse, finding that the addition of HF increased the toughness of the composites. Hamzaoui et al. [27] investigated HF- and carbon nanotube-blended mortars in terms of microstructure and mechanical behavior, observing increases of 10% and 24% in compressive and flexural strength, respectively, due to the combination of HF and carbon nanotubes.

Recent studies demonstrate the urgent need for environmentally friendly, high-performance building materials as an alternative to cement. While gypsum stands out with its advantages, such as low energy consumption and good fire resistance, its disadvantages, including its brittle nature and water sensitivity, limit its use, particularly in lightweight foam composites. While existing studies generally focus on gypsum alone or in combination with traditional reinforcement, there is a lack of comprehensive research on the synergistic system combining gypsum with foam technology, lightweight aggregates such as pumice, and natural fibers like hemp. The primary objective of this study is to address this scientific gap by developing a novel lightweight composite (GBFC) that

Table 1 Gypsum XRF results [28]

Oxide (%by mass)	CaO	SiO_2	Al_2O_3	Fe_2O_3	MgO	Na_2O	K_2O	SO_3	P_2O_5	TiO_2	LOI
Gypsum	33.6	2.1	0.6	0.3	0.7	0.1	0.2	42.4	0.3	0.4	19.2

Table 2 Technical specifications of gypsum [29]

Parameters	Reaction to fire	$CaSO_4$	Compressive strength	Flexural strength	Application temperature	Workability time	Setting time
Gypsum	A1	>%50	≥ 2 MPa	≥ 1 MPa	≥ 5℃	90–110 min.	180–220 min.

Table 3 Physical properties of foaming agent

Chemical composition	Synthetic liquid air entrainer
Appearance-Color	Translucent White Liquid
Density	130 g/L ± 2 gL
pH Value	5,0 ± 1
Chloride Content (Cl)	<%0,1
Alkali Content	<%5
Freezing Point	-5℃

combines gypsum binder, foam, pumice, and hemp fiber (HF), and to demonstrate the potential of this material through a comprehensive approach. The novelty of this study lies in presenting a cement-free, entirely gypsum-based foam composite formulation. It also utilizes hemp fiber, a sustainable natural fiber, to reduce the brittleness of gypsum and improve its mechanical performance. It also integrates pumice aggregate into the system to enhance its lightweight thermal performance. In this regard, the fresh state, physical, mechanical, thermal, and durability (high temperature resistance) properties of the composite were systematically examined, and a comprehensive answer was sought to the question of whether this innovative material could be a valid and sustainable alternative, especially for high-temperature-resistant non-bearing structural elements.

2 Materials and methods

2.1 Materials

Gypsum with a density of 2.32 kg/m³ was used as a binder to create a gypsum-based foam composite. XRF results and technical specifications of the gypsum used as a binder are given in Tables 1 and 2, respectively. Since the gypsum used in this study is in the form of hemihydrate ($CaSO_4·½H_2O$), it is seen in Table 1 that the LOI value is high. Fine-grained (0–4 mm) pumice with a 0.95 kg/m3 density was used as aggregate. The density of the foaming agent, whose physical properties are listed in Table 3, is ~130 g/L, accounting for 3% of the water mass used to produce the foam composite. The foam composite produced is reinforced with HF. The materials used in the study are given in Fig. 1.

2.2 Preparation of GBFC (gypsum-based foam composite)

Foam volumes of 20, 50, and 80 kg/m³ were selected as the unit weights, as GBFC targets are between 700 and 1200 kg/m³. The amount of gypsum used as a binder was determined to be 350 kg/m³. The water-to-binder ratio was determined to be 0.55 for all mixtures. The literature indicates that the water/binder ratio was between 0.65 and 0.70 for

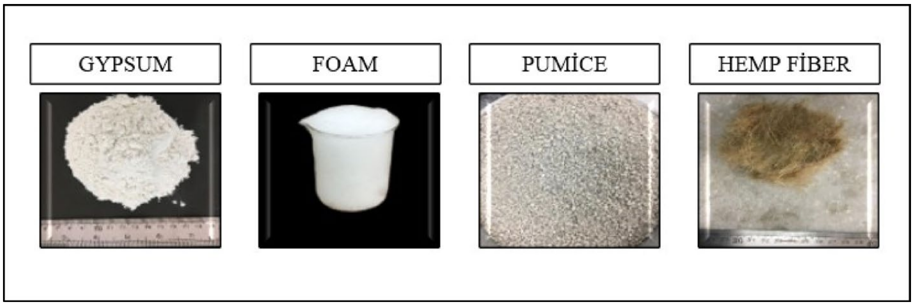

Fig. 1 Materials used in the study

Table 4 Material quantities (kg/m^3) of GBFC samples

Mix No.	Miz ID	Foam Vol. (kg/m^3)	HF (%)*	Gypsum	Pumice	Water	Foam	HF	Soaking water**
1	H0F20	20	0	350	477,7	192,5	20	0	238,8
2	H1F20		1	350	475,4	192,5	20	3,5	237,7
3	H2F20		2	350	473,2	192,5	20	7	236,6
4	H0F50	50	0	350	258,4	192,5	50	0	129,2
5	H1F50		1	350	256,2	192,5	50	3,5	128,1
6	H2F50		2	350	254,0	192,5	50	7	127,0
7	H0F80	80	0	350	39,2	192,5	80	0	19,6
8	H1F80		1	350	37,0	192,5	80	3,5	18,5
9	H2F80		2	350	34,8	192,5	80	7	17,4

*By volume

**Amount of water absorbed by pumice aggregate

similar studies [9, 28]. A lower water/binder ratio of 0.55 was selected for this study in contrast to the higher ratios documented in the literature. This was mainly due to the additional ready-mixed foam, which improved workability. The final product's superior qualities, including comparatively lower porosity and higher mechanical strength, were achieved through this addition, allowing for the use of less mixing water.

Hemp fiber (HF) was used at 0%, 1%, and 2% in the study. This length was chosen to achieve a homogeneous distribution by reducing the chance of agglomeration during mixing, while also effectively bridging cracks between the 0–4 mm pumice aggregate particles. The study found the maximum hemp fiber (HF) content to be 2%. This range was selected because the high water absorption capacity of the fibers causes the mixture to become much less workable as the fiber content increases. High fiber content can have a detrimental effect on compressive strength and increase the risk of clumping, according to published research. Gencel et al. [20] used the HF ratios of 0.75–1.5 and 3% in their study.

The mixtures were prepared using a 5-liter Hobart mixer. To prepare the mixture, first, gypsum and water were mixed for 2 min. Then, pumice aggregate was added, and the mixture was remixed for an additional 2 min. Then HF was added to the mixture and mixed for 2 min. The flow diameters of 25 strokes were measured on the flow table to determine the fresh state properties of the prepared mixtures. Specimens ready for molding were placed in 40 × 40 × 160 mm molds to decide on their mechanical and durability properties, and in 50 × 50 × 50 mm molds to determine their physical properties. The mixtures were removed from the mold after 24 h and stored for 14 days at a temperature of 30℃ and a relative humidity of 65%. The samples, which were kept for 14 days, were subjected to the desired experiments (Table 4).

2.3 Test methods

The flow diameters of GBFCs were measured in both the X and Y directions using a collapse funnel and flow table with a bottom diameter of 100 mm, an upper diameter of 70 mm, and a height of 60 mm, following the ASTM C1437 standard. The averages of these measurements were then calculated. Fresh unit weights were determined using 50 mm x 50 mm x 50 mm cube specimens according to ASTM C138 standards. The physical properties of GBFCs, including water absorption, apparent porosity, and unit volume weights, were determined using 50 mm x 50 mm x 50 mm specimens and the Archimedes method, as per the ASTM C642 standard. The flexural and compressive strengths of GBFCs were determined on day 14 using 40 mm x 40 mm x 160 mm prism specimens, as per ASTM C348 for flexural strength and ASTM C349 for compressive strength. To measure the high-temperature resistance of GBFCs, 40 × 40 × 160 mm prism specimens were used and heated to 250, 500, and 750℃ for 120 min at a heating rate of 10℃/min. The samples were cooled using the air cooling method, and mass losses and changes in mechanical properties were determined. Capillary water treatment depths were determined by performing capillarity tests on 50 mm × 50 mm × 50 mm cube specimens, in accordance with the ASTM C1585 standard. Samples with dimensions of 20 × 50 × 100 mm were used to measure the thermal conductivity of GBFCs according to the ASTM D7984-16 standard. All tests were performed in strict accordance with the procedures, sample preparation and instrument calibration steps defined in the relevant ASTM standards.

3 Results and discussions

3.1 Fresh properties

The workability and fresh-state images of Gypsum-Based Foam Composite (GBFC) mixtures, made with varying ratios of foam to hemp fiber, are shown graphically in Fig. 2. These pictures qualitatively demonstrate how the components of the mix affect workability. It is evident from looking at samples 1 through 9 in the figure that the foam content has a pronouncedly positive impact on workability. For instance, when comparing samples 1, 4, and 7, which contain no fiber, it is found that the mixture's spreading diameter increases significantly as the foam volume rises from 20 kg/m³ to 80 kg/m³. The extra volume of paste and the balling effect that the foam gives the mixture help to explain this. In contrast, the yield diameter seems to decrease as the hemp fiber content rises from 0% to 2% within each foam level (e.g., samples 1, 2, and 3). This decrease results from the fibers' absorption of the mixed water, which increases the mortar's viscosity and restricts its free movement. As a result, Fig. 2 illustrates the opposing effects of mix components on workability, providing visual evidence to support the quantitative yield diameter data presented in Fig. 3.

The flow diameters of the GBFCs, ranging from 212 to 288 mm, are illustrated in Fig. 3. When the foam volumes were kept constant, the increase in fiber volume resulted in a decrease in flow diameter. When the H0F20 mixture is compared with the H2F20 mixture in terms of flow diameter, it decreases by about 13.47%. Likewise, when the H0F80 mixture is compared with the H2F80 mixture in terms of flow diameter, it falls by approximately 11.80%. This is due to the water absorption property of HF. Gencel et al. [20] obtained similar results in their study, stating that the increase in HF decreased the flow diameters and was related to the water absorption properties of the HF used.

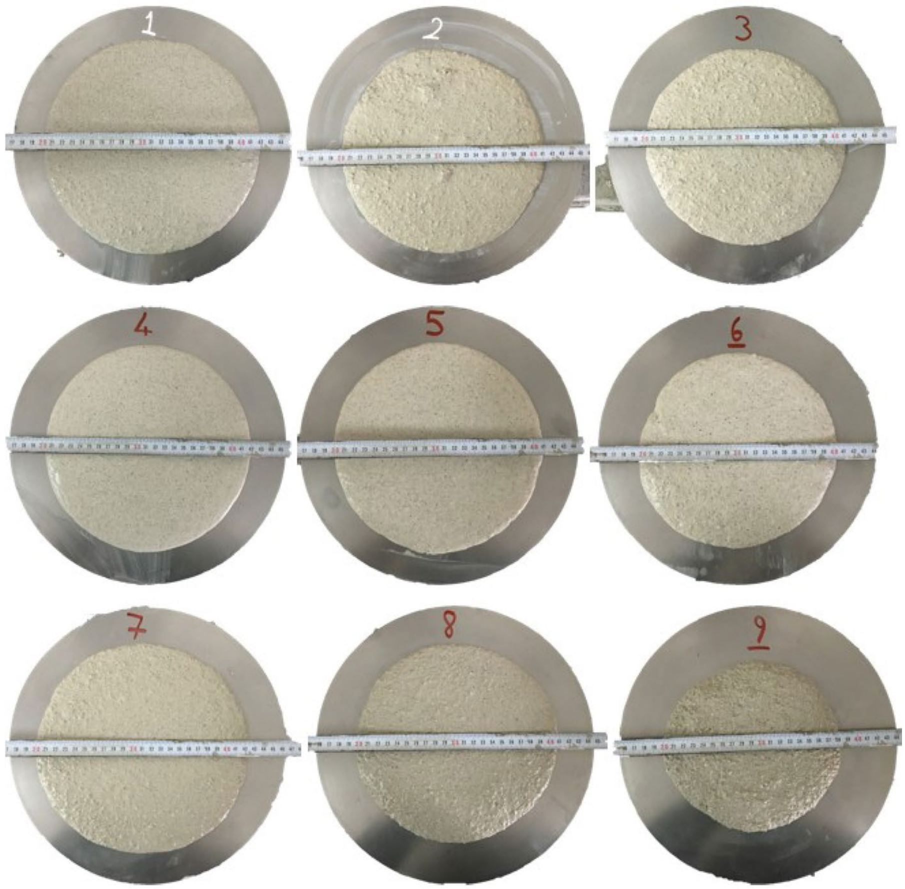

Fig. 2 Fresh state images of GBFCs

However, when the fiber volumes were kept constant, the increase in foam volume resulted in larger flow diameters. This is exemplified by an increase of approximately 17.55% when comparing the H0F20 mixture with the H0F80 mixture. Likewise, the H2F20 mixture showed an increase of about 19.81% compared to the H2F80 mixture. The increase in foam volume was effective in increasing the flow diameter. This can be explained by the fact that adding foam increases the paste volume by entraining air. It is also stated in the literature that increasing the foam volume enhances workability, as it increases the paste volume [30]. Ruano et al. [26] reported that HF actively interacts with fresh mortar, absorbing water from the fresh mix and reducing workability, thereby altering the hydration of the cement paste. Cho et al. [31] stated that they used fiber in foam concrete to address plastic shrinkage, crack control, capillary water treatment, and impact resistance. In addition, Kursuncu et al. and Gencel et al. stated in their studies that the foam volume increases viscosity values [32, 33].

The fresh unit volume weights of GBFCs determined with $50 \times 50 \times 50$ mm cube molds are given in Fig. 4. As seen in the figure, fresh unit weights vary between 797 and 1269 kg/m^3. In mixtures with foam volumes of 20 and 50 kg/m^3, the H2F20 and H2F50 mixtures have the lowest fresh unit volume weight. In contrast, the mixtures with the highest fresh unit volume weights were H1F20 and H1F80, with foam volumes of 20 kg/m^3 and 80 kg/m^3, respectively. Fresh unit volume weights are lighter than 1300 kg/m3 when all mixtures are evaluated. Regardless of the fiber volumes, when the foam

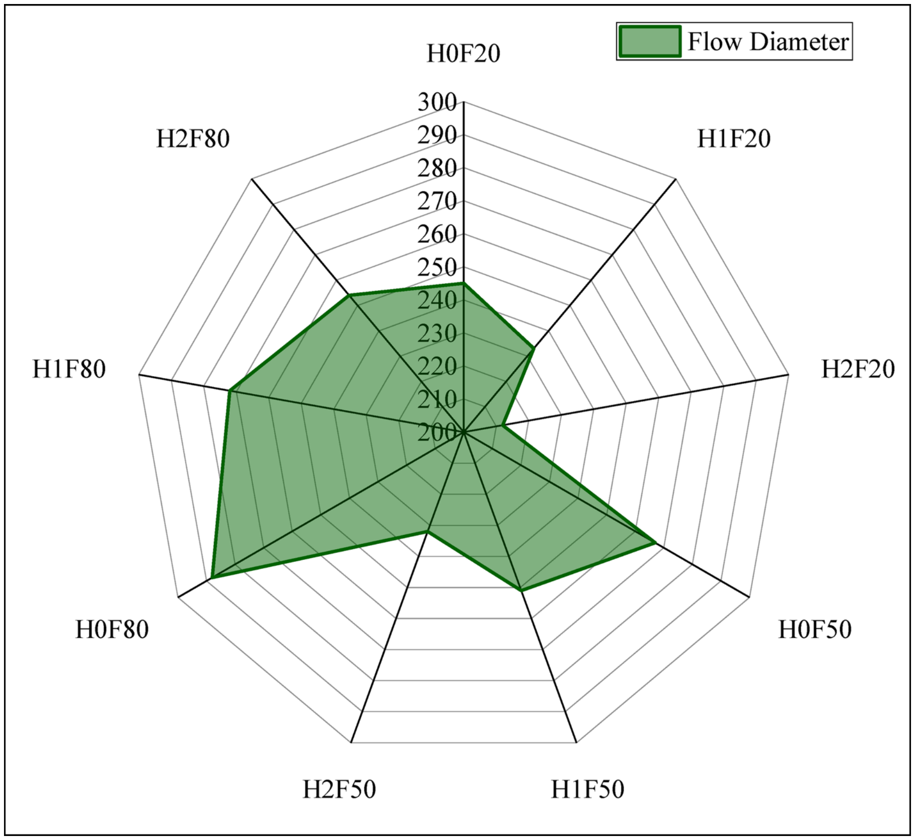

Fig. 3 Flow diameters (mm) of GBFCs

volumes are examined separately, they weigh approximately 1300 kg/m³ at a volume of 20 kg/m³, approximately 1000 kg/m³ at a volume of 50 kg/m³, and approximately 900 kg/m³ at a volume of 80 kg/m³. In this case, it was observed that the increase in foam volume decreased the fresh unit volume weight. Bayraktar et al. [34] found fresh unit volume weights of approximately 1500 kg/m³ in their HF study. This is explained by the lower fresh unit volume weights of GBFCs due to the lower specific gravity of gypsum compared to other binder materials, as observed in the study.

3.2 Physical properties

Fresh and dry unit volume weights of GBFCs are shown in Fig. 5. The lowest fresh unit weight was 797 kg/m³ in the H0F80 mixture, and the highest was 1269 kg/m³ in the H1F20 mixture. In dry unit weights, 723 kg/m³ was measured in the H0F80 mixture, and the highest was 1203 kg/m³ in the H1F20 mixture. When the foam amount is selected as 20 kg/m³, fresh unit weights range from 1269 to 1248 kg/m³, and dry unit weights range from 1203 to 1173 kg/m³ are observed. When the amount of foam is 50 kg/m³, a fresh unit weight ranging from 1013 to 895 kg/m³ and a dry unit weight ranging from 965 to 844 kg/m³ are observed. When the foam amount is selected as 80 kg/m³, fresh unit weights range from 797 to 924 kg/m³, and dry unit weights range from 723 to 887 kg/m³ are observed. Therefore, the increase in the amount of foam caused the sample to become lighter. This lightning may be due to the rise in microvoids in the microstructure of the specimens. Additionally, according to ACI 213R-14, the density range of semi-load-bearing lightweight concrete is between 800 kg/m³ and 1400 kg/m³. Since the dry

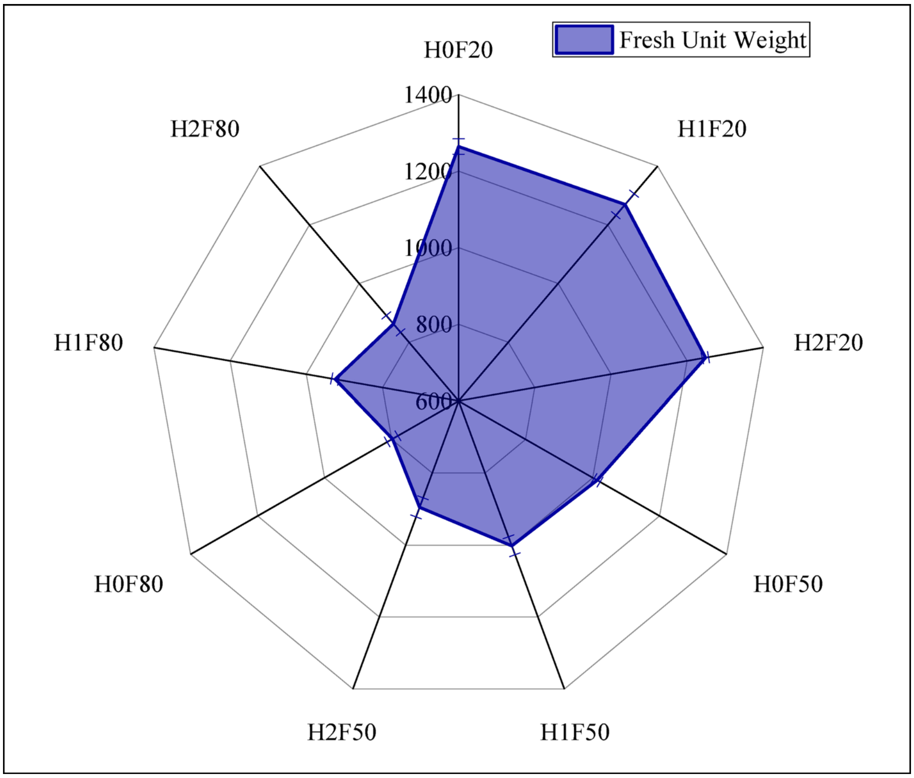

Fig. 4 Fresh unit weights (kg/m^3) of GBFCs

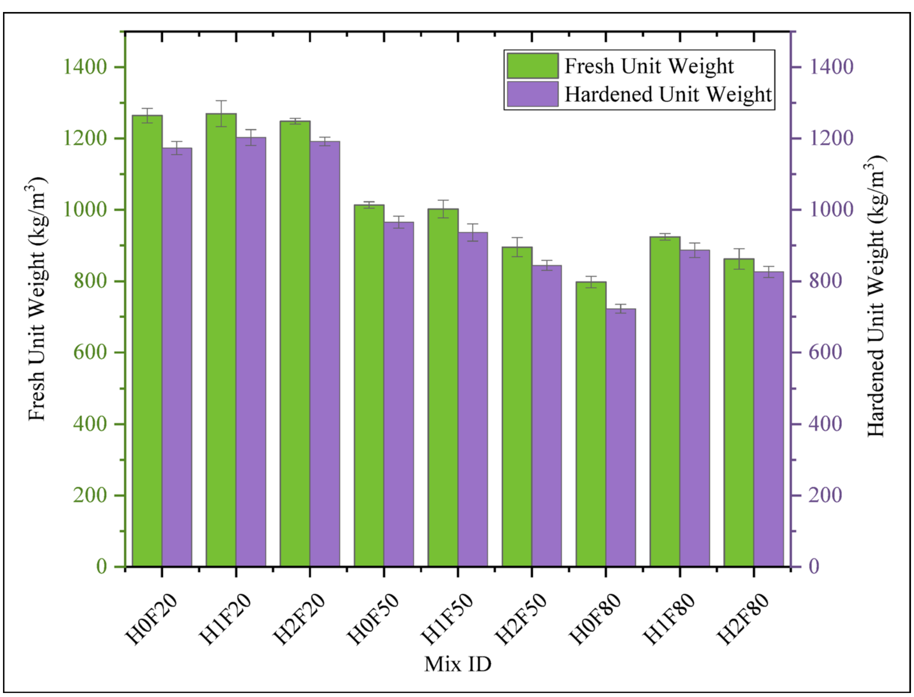

Fig. 5 Fresh and hardened unit weights of GBFC samples

unit weights of the specimens produced in this study ranged from 723 to 1203 kg/m³, they can be considered semi-load-bearing lightweight concrete according to ACI 213R-14 guidelines.

Figure 6 shows the apparent porosity and water absorption values of GBFCs in comparison. Porosity and water absorption values increased with increasing foam volume. Porosity and water absorption values increased with increasing foam volume. This is explained by the solid content decreasing as the foam volume increases [35]. In parallel with these explanations, the H0F80 mixture has the highest porosity and water absorption value. The lowest water absorption and porosity values are associated with the H1F20 mixture. When the fiber volume is kept constant in the mixtures and the foam volume increases, the apparent porosity also increases, resulting in higher water absorption values. Especially when the foam volume of 50 kg/m^3 was examined, the apparent porosity and water absorption values increased as the fiber volume increased. Increasing fiber volume decreases the workability, leading to an increase in porosity and water absorption values. In parallel with this situation in the literature, Babu et al. [36] stated in their study that water absorption percentages increase with increasing fiber volume. Likewise, Kaplan and Bayraktar [37] indicated in their research that the apparent porosity increased as the fiber ratio increased in the mixtures.

3.3 Mechanical properties

Figure 7 shows the flexural and compressive strengths of GBFCs in MPa units. When the flexural strengths are examined, it is observed that the flexural strength increases with an increase in fiber volume. This is explained by the fact that the fibers strengthen the GBFCs, which are more brittle due to the use of gypsum, thereby preventing crack propagation and increasing the flexural strength [38]. When the fiber volumes are kept constant and the foam volume increases, porosity increases, resulting in a decrease in

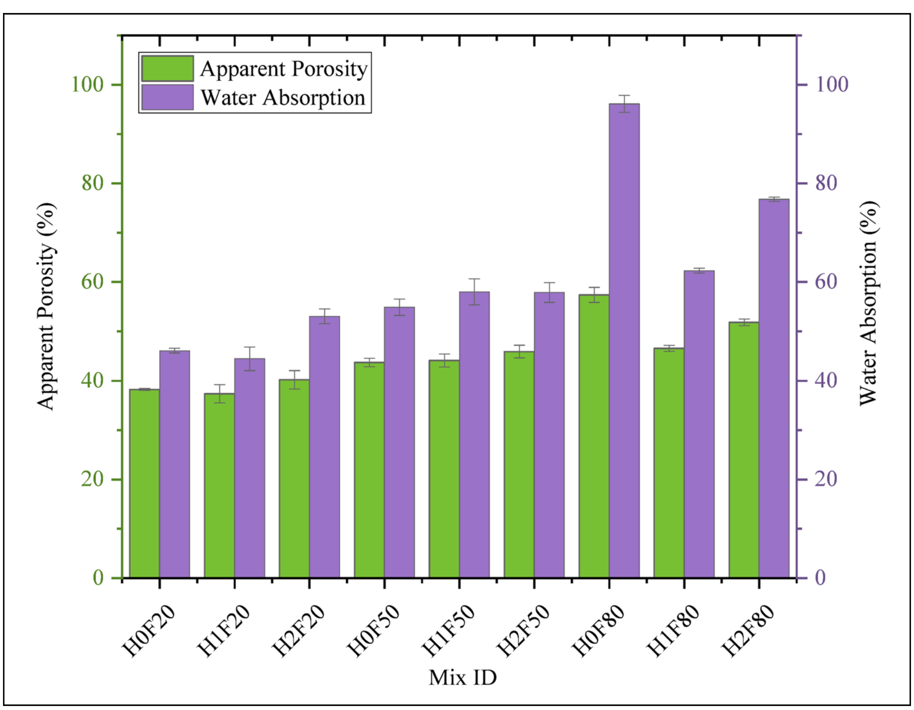

Fig. 6 Porosity and water absorption of GBFC samples

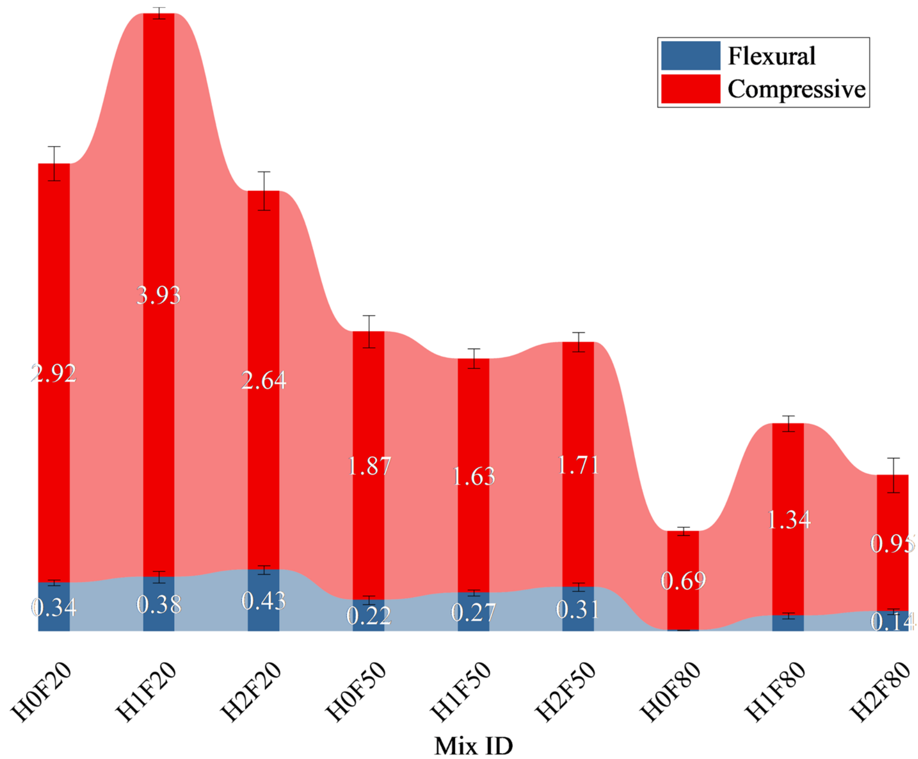

Fig. 7 Flexural and Compressive Strength (MPa)

flexural strength. However, when the foam volume is kept constant and the fiber volume rises, it is observed that the flexural strength increases. Therefore, the H2F20 mixture containing the highest fiber volume at the lowest foam volume shows the highest flexural strength.

In contrast, at the highest foam volume, the fiber-free H0F80 mixture exhibited almost no flexural strength. When 20 kg/m^3 was chosen as the foam volume and H_0F_{20} with 0% fiber volume was used as a reference, the H1F20 mixture showed an increase of approximately 11.76% and the H_2F_{20} mixture showed an increase of roughly 26.47% in flexural strength. In their study, Page et al. [39] reported that flexural strength increased with increasing flax fiber ratio. Boulekbache et al. [40] also stated that the mixture's consistency affects the fiber position, which in turn affects the flexural strength.

When the compressive strengths were analyzed, the highest strength was obtained with the H1F20 mixture. The lowest compressive strength was obtained with the H0F80 mixture. When the whole mixture was analyzed, compressive strengths decreased with increasing foam volume. Compressive strengths decreased when the fiber volume was kept constant and the foam volume increased. Taking the H0F20 mixture as a reference, the H0F50 and H0F80 mixtures decreased by 35.95% and 76.36% respectively. Taking the H1F20 mixture as reference, the H1F50 and H1F80 mixtures decreased by 58.52% and 65.90%, respectively. Likewise, when the H2F20 mixture was taken as a reference, H2F50 and H2F80 mixtures decreased by 35.22% and 64.01%, respectively. This way, when each fiber volume ratio is evaluated within itself and the compressive strength reduction percentages are compared, the compressive strength reduction percentages decrease with increasing fiber volume ratio. At 20 and 80 kg/m^3 foam volumes, the highest strengths were obtained with 1% fiber volumes. Mahdi [41] stated that the reason for this situation is the inability of the matrix to penetrate between the fibers due to the increase in viscosity during matrix mixing in macro fiber additions, the decrease in fiber wetting before the matrix hardens, and the decline in adherence (weaker interface) between the matrix and fibers. Page et al. [39] obtained a similar result, explaining that the compressive strengths of mixtures with 2% and 3% fiber content decreased due to high porosity values. Jaber [42] stated that adding HF would be responsible for increases in the compressive strength of the specimens as it increases the toughness of the mortars and makes the composites more resistant to tensile stress, thereby increasing the compressive strength of the mortar specimens.

Figure 8 shows the correlation between the flexural and compressive strengths of GBFCs. As can be seen from the graph, the flexural strength increases with the increase in compressive strength. This correlation is supported by the coefficient $R^2 = 0.81$.

Figure 9 shows the correlation between compressive strength, hardened unit weight and apparent porosity of GBFCs. As shown in the figure, the apparent porosity decreased as the compressive strength increased. The lower porosity, i.e., void ratio, provided a higher compressive strength. Additionally, the correlation coefficient between compressive strength and apparent porosity yields a high value of $R^2 = 0.95$, indicating a strong relationship. On the other hand, there is a strong correlation between compressive strength and hardened unit weight, as noted in the R^2 value of 0.88. The increase in hardened unit weight also corresponded to an increase in compressive strength. Especially mixtures with a unit weight of more than 1000 kg/m³ have a compressive strength exceeding 2.5 MPa.

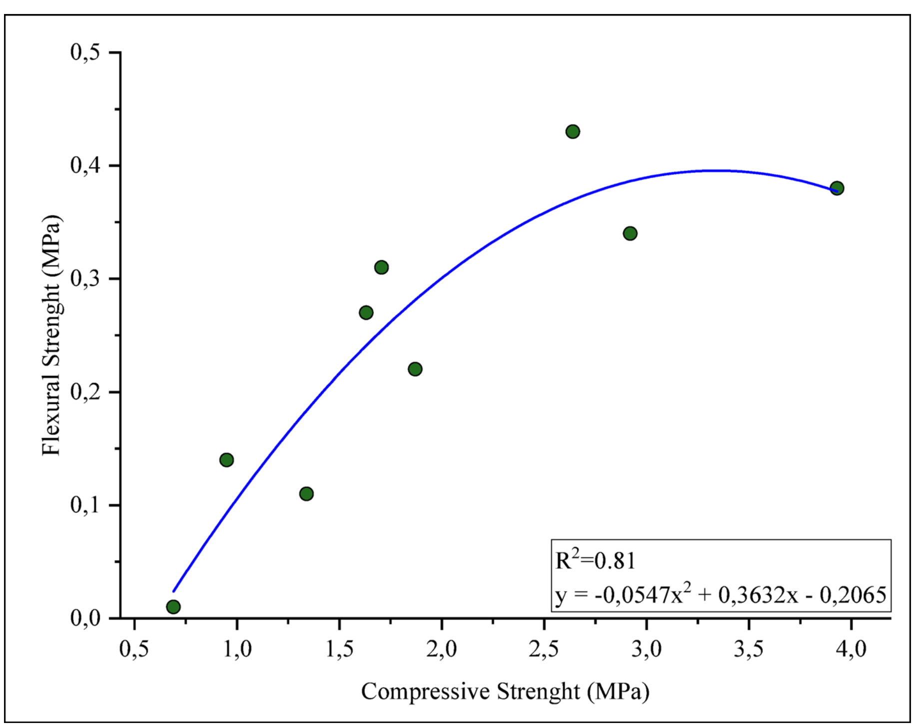

Fig. 8 Correlation between flexural and compressive strength

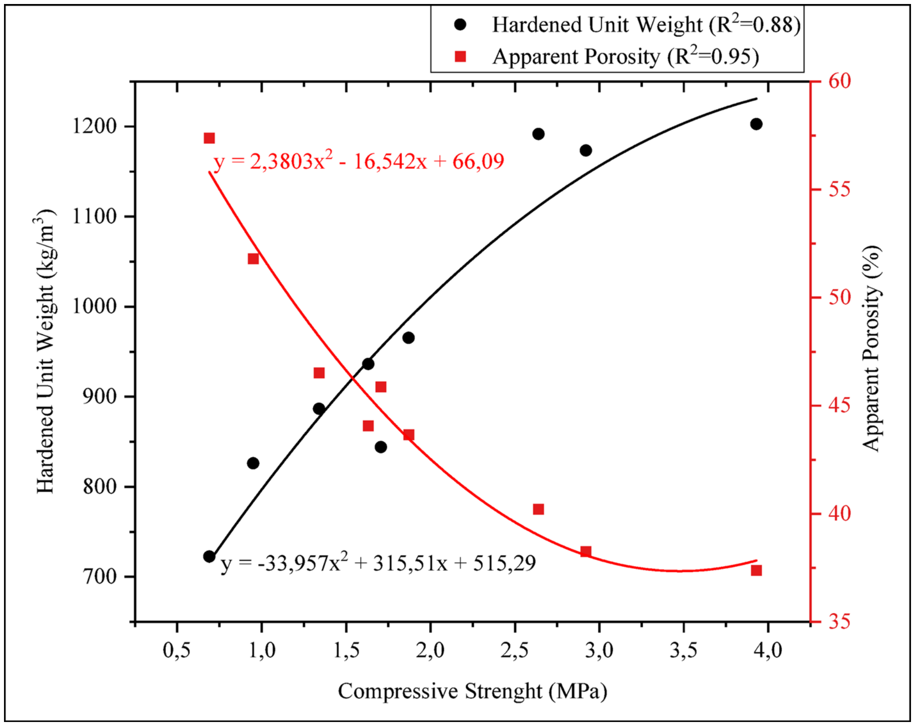

Fig. 9 Correlation between compressive strength, hardened unit weight and apparent porosity

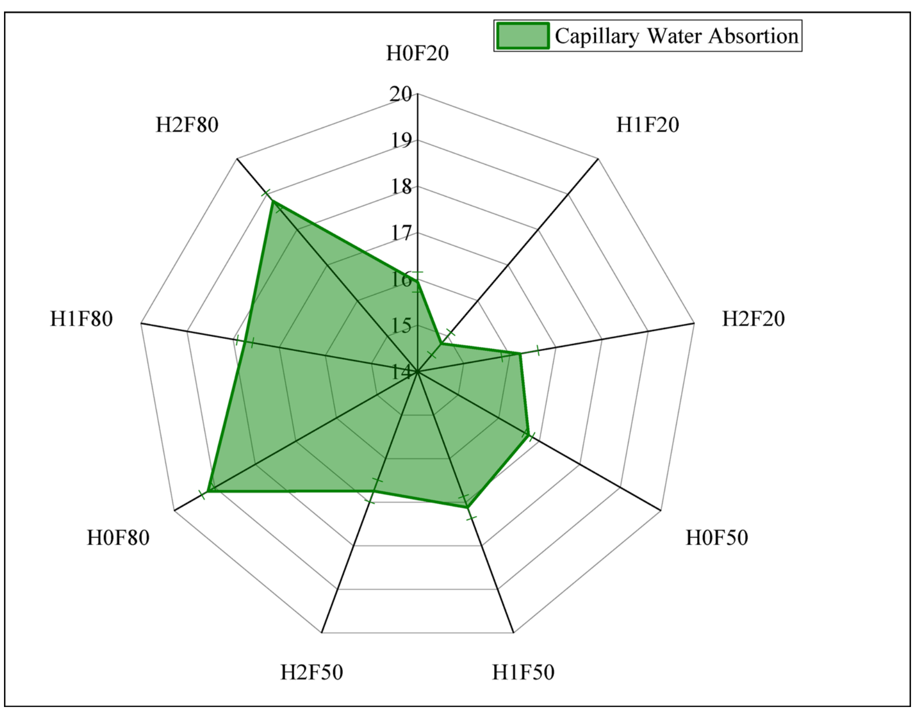

Fig. 10 Capillary water absorption (kg/m^2) of GBFS samples

3.4 Water treatment depth

Capillary water treatment depths of GBFCs are shown in kg/m^2 units in Fig. 10. Capillary water treatment depth refers to the capacity of a medium to transport (absorb) a liquid through capillarity [43]. The highest water treatment depth of GBFCs is associated with the H0F80 mixture, while the lowest water treatment depth is related to the H1F20 mixture. As shown in the figure, the depth of capillary water treatment increased with increasing foam volume. The increase in capillary water treatment depth was attributed to the mixture's increased porosity and air void content, along with higher foam content, which led to a more connected pore network, as reported in previous studies. Gencel et al. stated in their research that increasing the foam volume in foam concrete increases the capillary water treatment depth due to a decrease in solid content and an increase in porosity. Benli reported similar results to those of Karahan et al. and Shaikh et al. When the mixtures with a 20 kg/m^3 foam volume are analyzed, the lowest capillary water treatment depth is associated with the H1F20 mixture, while the highest value is related to the H2F20 mixture. When the mixtures with a 50 kg/m^3 foam volume are analyzed, the lowest value belongs to the H0F50 mixture, and the highest value belongs to the H1F50 mixture. When the mixtures with a foam volume of 80 kg/m^3 are analyzed, the lowest value corresponds to the H1F80 mixture, and the highest value corresponds to the H0F80 mixture. Similar results were observed in a study conducted by Bayraktar and colleagues. In this study, it was reported that when 2% basalt fibre was used in foam concrete mixtures with a foam volume of 50 kg/m^3, there was an approximately 32% increase in capillary water treatment depth values [44]. They attributed this increase in capillary water treatment depth to the lower surface adherence of basalt fibers to the cement paste, which increased the capillary water transport of the concrete medium.

Figure 11 shows the correlation plot between the compressive strength and the depth of capillary water treatment for GBFCs. We have stated that the compressive strength increases with a decrease in porosity. Consequently, with an increase in compressive strength, the hollow structure will decrease, and the capillary water absorption values will also decrease. This prediction is supported by a correlation coefficient of R^2 = 0.95

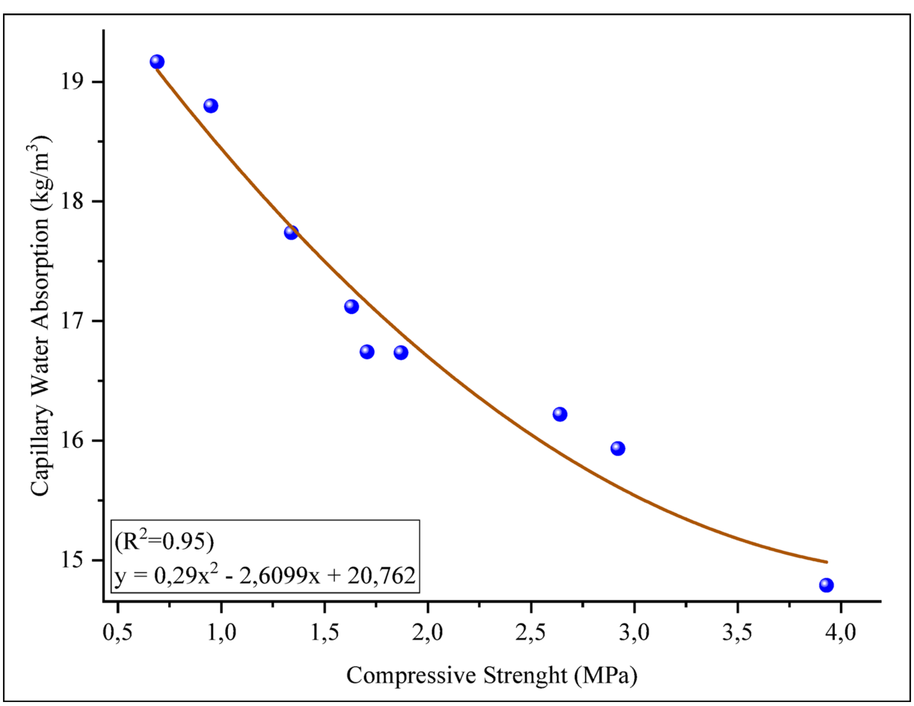

Fig. 11 Correlation between compressive strength and depth of capillary water treatment

for compressive strength and capillary water absorption. From all this, the highest compressive strength means the lowest depth of capillary water treatment.

3.5 High-temperature resistance

Figure 12 shows the mass loss of GBFCs after high-temperature treatment in percentage terms. Mass loss is another variable often calculated to understand the overall physical property changes of concrete subjected to deforming factors [33]. As shown in the figure, mass losses increase with increasing temperature. It is understood that similar results were obtained when compared with the results of the study conducted by Gencel et al. [35]. For example, when the H0F20 mixture is examined, the mass loss percentage differences at 500℃ and 750℃ are 3.08% and 6.35%, respectively, compared to the reference at 250℃. When the H1F50 mixture is examined, the mass loss percentage differences at 500℃ and 750℃ are 2.95% and 6.84%, respectively, when compared to the reference at 250℃. When the H2F80 mixture is examined, the mass loss percentage differences at 500℃ and 750℃ are 6.15% and 9.09%, respectively, when compared to the reference at 250℃. Similarly, mass losses increase with increasing foam volume. Nambiar et al. stated in their study that this increase in mass loss is due to a decrease in the volume of available loss materials based on internal stresses caused by exposure to high temperatures [45]. For example, when H0F20 is considered as the reference for 250℃, the mass loss percentage differences of H0F50 and H0F80 mixtures are 0.72 and 0.91, respectively. Similarly, when H1F20 is taken as a reference for 500℃, the mass loss percent differences of H1F50 and H1F80 mixtures are 0.47 and 2.45, respectively. Likewise, when the H2F20 mixture is considered as the reference for 750℃, the mass loss percent differences of the H2F50 and H2F80 mixtures are 1.12% and 2.95%, respectively. Increasing

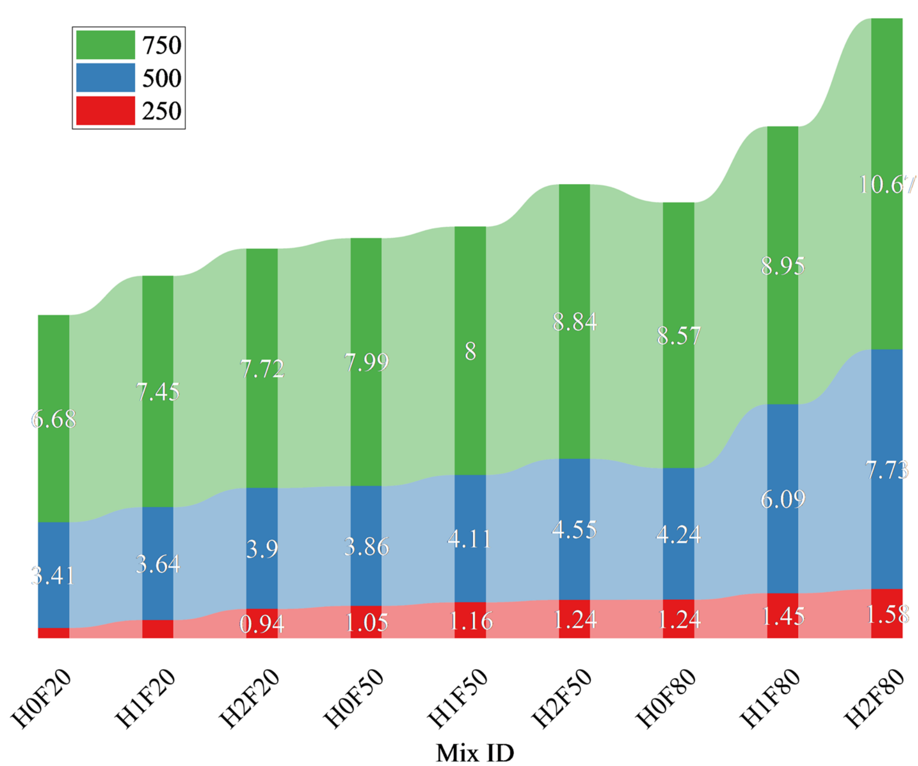

Fig. 12 Mass loss (%) of GBFS samples

the fiber volume of AECBs is also observed to increase mass losses. For example, when the foam volume of 80 kg/m³ at 500℃ is examined, with 0% fiber volume as the reference, the mass loss percentage differences for 1% and 2% fiber volume are observed to be 1.85% and 3.49%, respectively. Since HF is an organic-based fiber, it burns when exposed to high temperatures. It is believed that these fiber volumes are replaced by voids after exposure to high temperatures in GBFC, thereby increasing mass loss.

Figure 13 shows the percentages of UPV change after exposure to different high temperatures for GBFCs. UPV is a non-destructive test widely applied to assess internal defects of concrete specimens, especially after exposure to deteriorating conditions [46]. Many studies have also indicated that high temperatures cause significant damage to the microstructure [47, 48]. As the figure shows, UPV change percentages increase as the temperature values increase. The blend showing the highest UPV change after 250℃ high temperature is H1F80, and the blend showing the lowest UPV change is H0F20. When 500℃ is analyzed, the highest change belongs to H1F50 and H2F80 mixtures, while the lowest change belongs to H2F20. When examined at 750℃, the highest change is observed in the H1F80 mixture, and the slightest change is observed in the H2F20 mixture. When each high-temperature value is analyzed separately, the average percentages of UPV change for 250℃, 500℃, and 750℃ are 12.27%, 46.02%, and 55.02%, respectively. It was observed that the increase in the percentages of change in UPV with increasing temperature value is due to the results of Bayraktar et al. [44]. This is due to the microstructural degradation of the mixtures exposed to higher temperatures [49, 50]. When the GBFCs were analyzed, the UPV change percentages generally increased with the increase in foam volume. The larger reductions in UPV of mixtures with higher

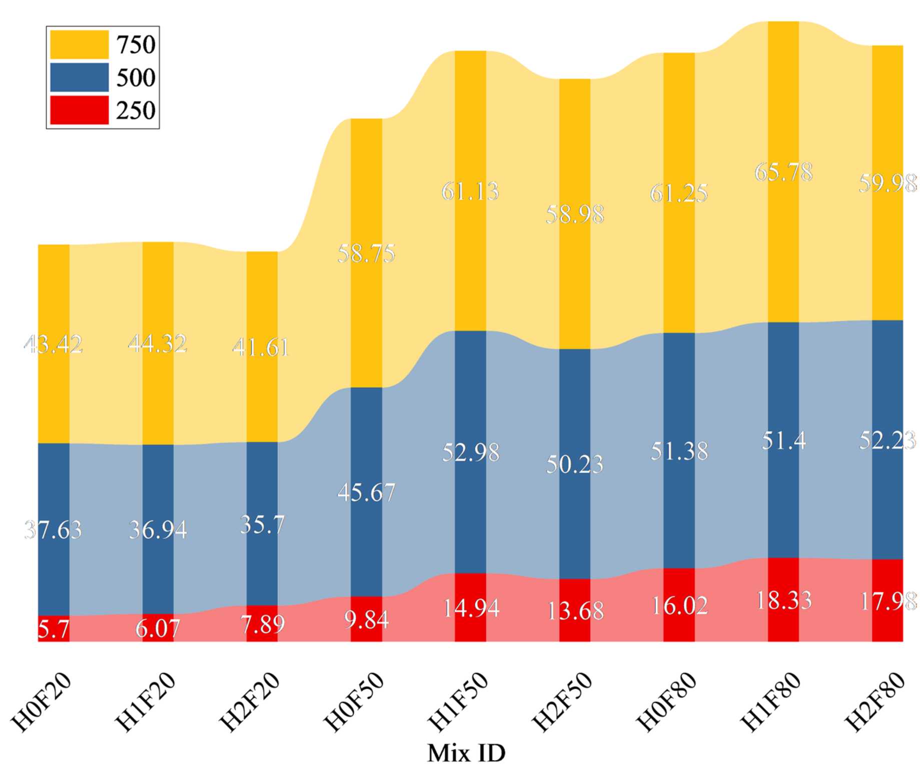

Fig. 13 UPV changes (%) of GBFS samples

foam volumes are consistent with previous studies. They are attributed to the increased porosity of the mixtures, allowing UPV to move more slowly [49, 50].

Figure 14 shows the correlation between the percentages of mass loss and UPV change after 250℃ high temperature for GBFCs. As the percentage of mass loss decreases, UPV change also decreases. The coefficient R^2 = 0.87 indicates that this correlation is quite strong.

Figure 15 shows the post-high-temperature compressive strength comparison of GBFCs in MPa units. H1F20 mixture showed the highest compressive strength at 14 days and at other high temperatures. As the high-temperature value increased, compressive strengths decreased. Regarding the 14-day compressive value of the H2F20 mixture, the compressive strength reduction percentages for 250℃, 500℃, and 750℃ are 1.71%, 23.63%, and 58.56%, respectively. Regarding the 14-day compressive value of H1F50 mix, the percentages of compressive strength reduction at 250℃, 500℃, and 750℃ are 4.90%, 33.12%, and 73.61%, respectively. Likewise, when the 14-day compressive value of the H0F80 mixture is taken as a reference, the percentages of compressive strength reduction for 250℃, 500℃, and 750℃ are 4.34%, 50.72%, and 85.50%, respectively. As can be understood from the values, both the increase in temperature and the increase in foam volume decrease the compressive strength. The average compressive strength after 250℃ is 1.84 MPa, after 500℃ is 1.33 MPa and after 750℃ is 0.66 MPa. Strength losses are attributed to an intrinsic degradation mechanism caused by high temperatures, which includes the loss of free and microstructural water, ultimately leading to paste disintegration [51]. In their study, Gencel et al. [33] reported that compressive strengths decreased after exposure to high temperatures, with increasing foam volume. The high strength loss experienced in mixtures with higher foam volumes is due to the reduction

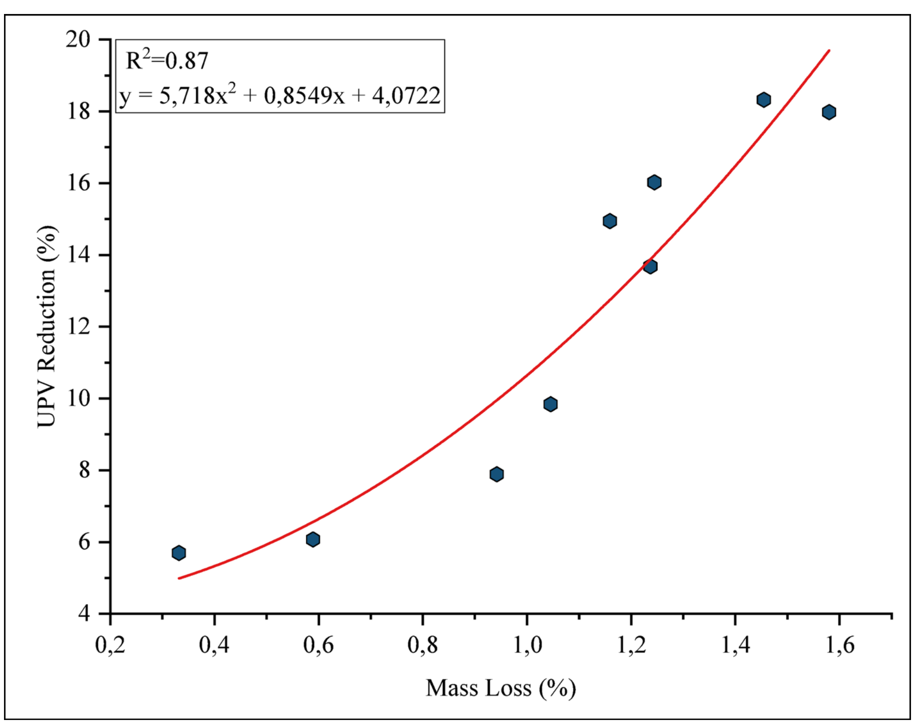

Fig. 14 Correlation of percent mass loss and percent UPV change at 250℃

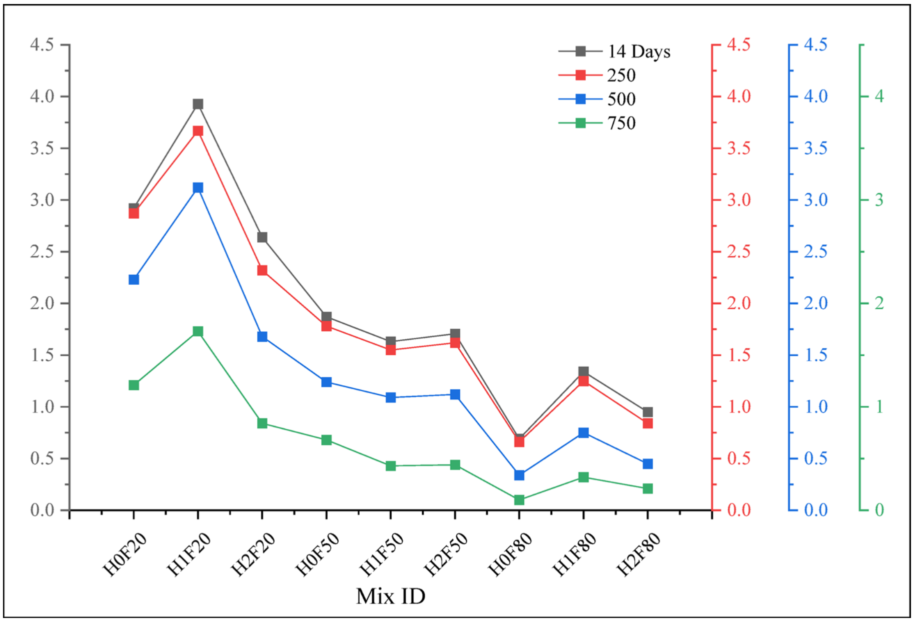

Fig. 15 Compressive strength (MPa) of GBFS specimens after high temperature

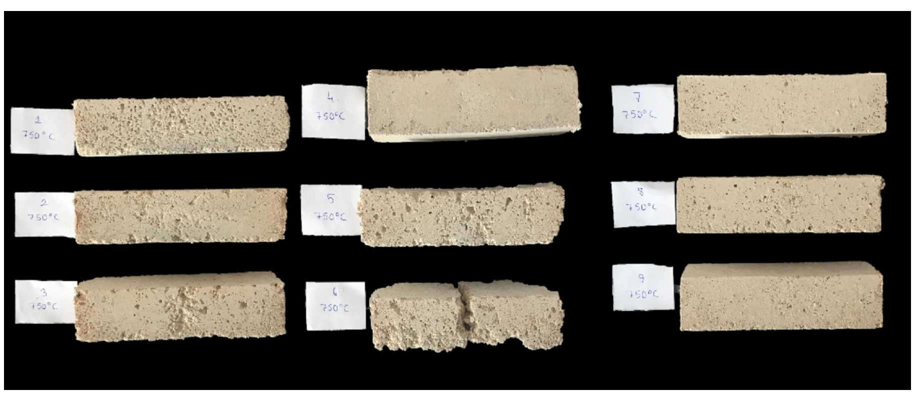

Fig. 16 Views of GBFCs after high temperature

in the content of solid materials resulting from the thermal stresses to which they are exposed [45].

Figure 16 shows the general appearance of GBFC specimens after 750 °C. It is observed that there is minimal damage to the specimens. In the picture, it is observed that there is relatively more damage in mixture number 6 (H2F50). The H2F50 mixture exhibits one of the lowest mechanical properties after exposure to high temperatures. Therefore, some minor damage was observed in this mixture due to high temperatures.

3.6 Thermal conductivity

Thermal conductivity coefficients of GBFCs are shown in W/m.K in Fig. 17. As seen in the figure, thermal conductivity decreased with increasing foam volume. When the foam volumes are analyzed separately, the average thermal conductivity coefficient of 20 kg/m^3 volume is 0.323 W/m.K, the average coefficient of 50 kg/m^3 volume is 0.314 W/m.K and the average coefficient of 80 kg/m^3 volume is 0.303 W/m.K. Capasso et al. [52] stated that their data indicate that foam volume has a significant effect on thermal conductivity

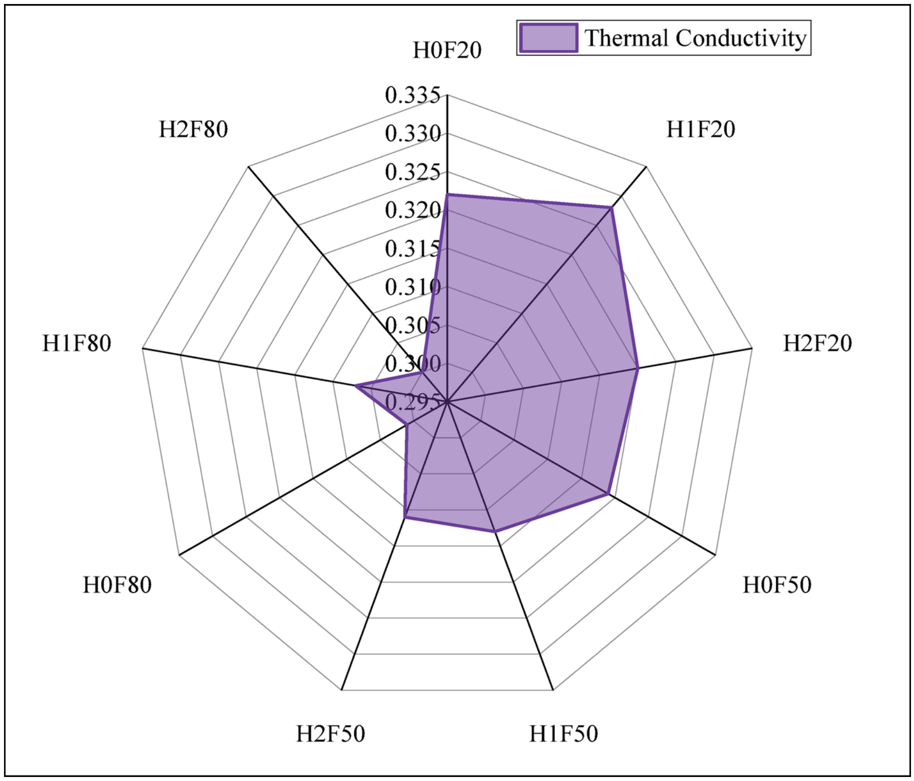

Fig. 17 Thermal conductivity coefficients (W/m.K) of GBFS specimens

and that a proportionality directly relates them. They also noted that, as expected from the literature, a decrease in thermal conductivity is observed for lower densities, because air has lower thermal conductivity than solids [53, 54]. Since the thermal conductivity resistances of gypsum and foam concrete are high, very low coefficients were obtained. When each foam content was examined separately, the 2% HF content blends showed the lowest coefficients of variation. In parallel with the findings, Ghalieh et al. stated that natural fibers improve the thermal insulation properties of concrete by reducing the thermal conductivity coefficient.

Figure 18 shows the correlation between thermal conductivity, hardened unit weight and apparent porosity of GBFCs. As the porosity, i.e., void ratio, decreased, the thermal conductivity coefficient increased. As can be seen from the correlation coefficient (R^2 = 0.86), this correlation is highly significant. The thermal conductivity coefficient increased as the unit volume increased. $R^2 = 0.79$ supports this close correlation. Porosity and hardened unit weight show an inverse relationship to thermal conductivity. As the hardened unit weight of GBFS specimens increases, the porosity decreases and therefore, the coefficient of thermal conductivity increases.

3.7 Microstructure analysis

Microstructural pictures of the H2F20 sample with 2% HF are shown in Fig. 19. A dense and well-crystallized gypsum matrix is visible in the pictures. The matrix appears to be composed of large, elongated (lath-like), interlocking calcium sulfate crystals in the high-magnification (left) image. Smaller, blocky, prismatic gypsum crystals fill the spaces and surroundings of this main skeletal structure, forming a dense structure. The leading

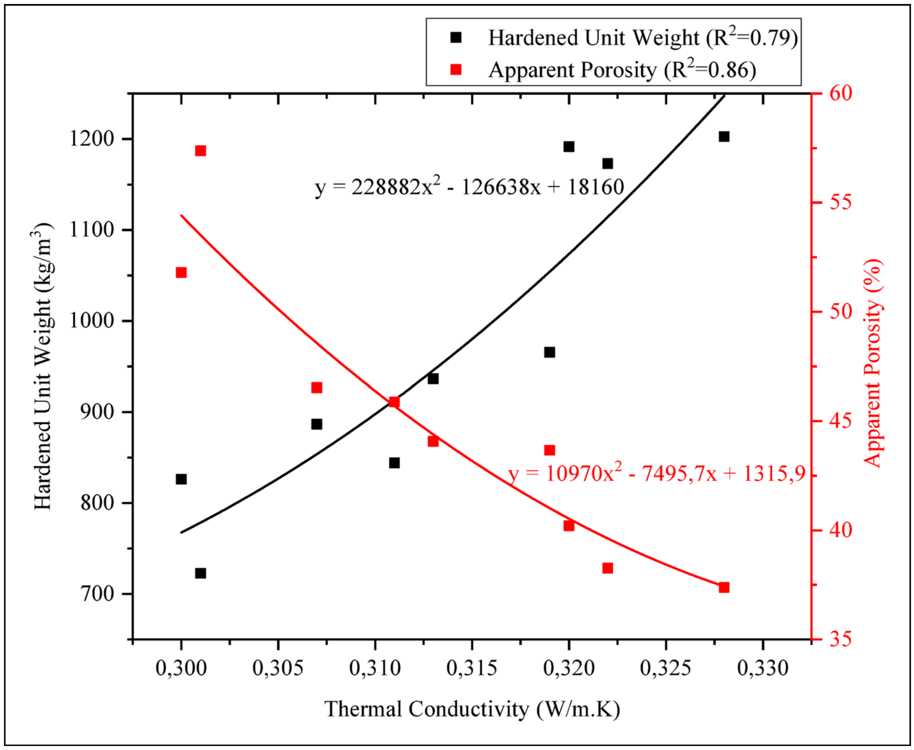

Fig. 18 Correlation of thermal conductivity, hardened unit weight and apparent porosity

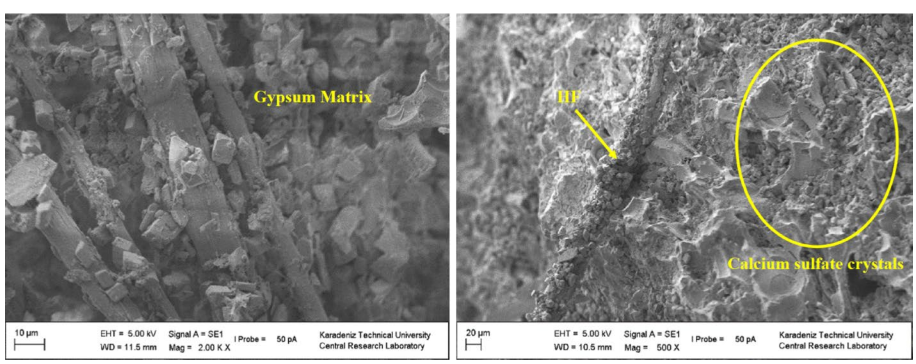

Fig. 19 SEM images of H2F20 mixture

cause of the composite's 2.64 MPa compressive strength is its thick, interlocking crystal structure.

Hemp fiber (HF) is also visible embedded in this dense matrix in the low-magnification (right) image. The development of crystals surrounding the fiber results in a strong mechanical interlocking between the fiber and matrix. The high flexural strength of 0.43 MPa in this sample's series can be attributed to its robust interface and the fibers' ability to crack-bridge. In summary, microstructural analyses confirm that the H2F20 sample's superior mechanical performance is due to the combination of a dense, tightly packed gypsum matrix and the efficient operation of hemp fiber reinforcement within this matrix.

4 Conclusions

This study used gypsum binder, pumice aggregate, foam, and hemp fiber (HF) as a sustainable cement substitute to successfully develop a new gypsum-based foam composite (GBFC) and thoroughly characterize its performance. The results demonstrate the material's characteristics and potential resulting from the combination of these special elements. It was found that the primary factor influencing the composite's physical characteristics was its foam content. As anticipated, increasing the foam volume from 20 kg/m³ to 80 kg/m³ resulted in a significant decrease in the material's unit weight (down to 723 kg/m³), while also increasing the material's apparent porosity (up to 57.8%) and water absorption capacity (up to 96.14%). By reducing the material's thermal conductivity, this increased porosity enhanced the insulation's performance.

Mechanical performance suffered as a result of these physical property gains; higher foam and porosity decreased flexural and compressive strengths. The importance of hemp fiber (HF) reinforcement became clear at this point. By improving the brittle structure of the gypsum matrix, HF's fiber-bridging mechanism significantly increased flexural strength. The H2F20 mixture, which contained 20 kg/m³ foam and 2% HF, had the highest flexural strength (0.43 MPa). The H1F20 mixture, which was also produced with a lower foam content (20 kg/m³) and 1% HF, showed the best performance in terms of compressive strength (3.93 MPa).

The potential of the created composite was validated through durability analyses, particularly in terms of its high-temperature performance. The samples showed remarkable residual compressive strength (up to 1.73 MPa at the lowest foam ratio) and retained their structural integrity even after being exposed to temperatures as high as 750 °C. This outcome demonstrated that the foam composite structure effectively leverages the well-known fire-resistant properties of pumice and gypsum.

In summary, this study demonstrates that GBFC is a promising, sustainable, and practical building material, particularly for applications such as non-load-bearing, fire-resistant partition walls, due to its low unit weight (range: 723–1203 kg/m³), high temperature resistance, and low thermal conductivity. A foam content of 20 kg/m³ and a hemp fiber content of 1%–2% produced the best mechanical and physical balance.

It is recommended that future research focus on a few key areas in light of the study's findings. To enhance the gypsum matrix's resistance to water, the effects of mineral additives such as fly ash or slag should be investigated. To further understand the material's behavior under realistic environmental conditions, long-term durability tests, such as freeze-thaw cycles, should be conducted. Additionally, the material's sound insulation qualities should be investigated, as these are crucial for applications involving non-load-bearing walls. These will be essential steps in bringing this promising material to the real world.

Author contributions

Burak Bodur: Methodology, Writing – review & editing. Validation, Data curation Oguzhan Yavuz Bayraktar: Sample collection, Validation, Data analysis, Methodology Gokhan Kaplan: Supervision, Conceptualization, Project administration.

Funding

The authors declare that no funds, grants, or other support were received during the preparation of this manuscript.

Data availability

The datasets generated during and/or analyzed during the current study are available from the corresponding author onreasonable request.

Declarations

Ethics approval and consent to participate
Not applicable.

Consent for publication
Not applicable.

Competing interests
The authors declare no competing interests.

Received: 24 May 2025 / Accepted: 10 September 2025
Published online: 29 September 2025

References

1. Kaya M, İlkentapar S, Durak U, Atabey İİ, Çelikten S. Physical mechanical and microstructural properties of Kaolin-Based fly Ash-Added geopolymer mortars. Iran J Sci Technol Trans Civ Eng. 2024;48:3559–72. https://doi.org/10.1007/s40996-024-01396-8.
2. Yurt Ü, Bekar F. Comparative study of hazelnut-shell biomass Ash and Metakaolin to improve the performance of alkali-activated concrete: A sustainable greener alternative. Constr Build Mater. 2022;320:126230. https://doi.org/10.1016/j.conbuildmat.2021.126230.
3. Dokuzlar G, Dündar B, Yurt Ü. Effect of recycled asphalt waste on mechanical properties of alkali-activated mortars. Proc Inst Mech Eng Part E J Process Mech Eng. 2024;238:1851–9. https://doi.org/10.1177/09544089231191621.
4. Li M, Tan H, He X, Jian S, Li G, Zhang J, Deng X, Lin X. Enhancement in compressive strength of foamed concrete by ultra-fine slag. Cem Concr Compos. 2023;138:104954.
5. Honglei C, Zuquan J, Tiejun Z, Benzhen W, Zhe L, Jian L. Capillary Suction induced water absorption and chloride transport in non-saturated concrete: the influence of humidity, mineral admixtures and sulfate ions. Constr Build Mater. 2020;236:117581.
6. Cong X, Qiu T, Xu J, Liu X, Wang L, Wang Y, Chen C, Zhao L, Xing C, Tan Y. Study on the effectiveness of fibre reinforcement on the engineering performance of foamed concrete, case stud. Constr Mater. 2022;16:e01015.
7. Amran YM, Farzadnia N, Ali AA. Properties and applications of foamed concrete; a review. Constr Build Mater. 2015;101:990–1005.
8. Zhang Z, Provis JL, Reid A, Wang H. Mechanical, thermal insulation, thermal resistance and acoustic absorption properties of geopolymer foam concrete. Cem Concr Compos. 2015;62:97–105.
9. Gawlicki M. Gypsum–another approach, Cem. Wapno Beton. 2009;14:86–96.
10. Li Z, Wang X, Yan W, Ding L, Liu J, Wu Z, Huang H. Physical and mechanical properties of gypsum-based composites reinforced with basalt, glass, and PVA fibers. J Build Eng. 2023;64:105640.
11. Du Z, She W, Zuo W, Hong J, Zhang Y, Miao C. Foamed gypsum composite with heat-resistant admixture under high temperature: mechanical, thermal and deformation performances. Cem Concr Compos. 2020;108:103549.
12. Thomas G. Thermal properties of gypsum plasterboard at high temperatures. Fire Mater. 2002;26:37–45.
13. Sun H, Qian J, Yang Y, Fan C, Yue Y. Optimization of gypsum and slag contents in blended cement containing slag. Cem Concr Compos. 2020;112:103674. https://doi.org/10.1016/j.cemconcomp.2020.103674.
14. Santos T, Gomes MI, Silva AS, Ferraz E, Faria P. Comparison of mineralogical, mechanical and hygroscopic characteristic of earthen, gypsum and cement-based plasters. Constr Build Mater. 2020;254:119222. https://doi.org/10.1016/j.conbuildmat.2020.119222.
15. Rovero L, Galassi S, Misseri G. Experimental and analytical investigation of bond behavior in glass fiber-reinforced composites based on gypsum and cement matrices. Compos Part B Eng. 2020;194:108051. https://doi.org/10.1016/j.compositesb.2020.108051.
16. Park S-H, Manzello SL, Bentz DP, Mizukami T. Determining thermal properties of gypsum board at elevated temperatures. Fire Mater. 2010;34:237–50.
17. Ghazi Wakili K, Hugi E, Wullschleger L, Frank TH. Gypsum board in fire—modeling and experimental validation. J Fire Sci. 2007;25:267–82.
18. Rahmanian I, Wang YC. A combined experimental and numerical method for extracting temperature-dependent thermal conductivity of gypsum boards. Constr Build Mater. 2012;26:707–22.
19. Li Z, Wang X, Zhu Z, Wu Z. Effect of mixing methods on the dispersion of fibers in the gypsum matrix and performance improvement mechanism. Constr Build Mater. 2022;320:126193. https://doi.org/10.1016/j.conbuildmat.2021.126193.
20. Gencel O, Yavuz Bayraktar O, Kaplan G, Benli A, Martínez-Barrera G, Brostow W, Tek M, Bodur B. Characteristics of hemp fibre reinforced foam concretes with fly Ash and Taguchi optimization. Constr Build Mater. 2021;294:123607. https://doi.org/10.1016/j.conbuildmat.2021.123607.
21. Sarasini F, Tirillò J, Sergi C, Seghini MC, Cozzarini L, Graupner N. Effect of basalt fibre hybridisation and sizing removal on mechanical and thermal properties of hemp fibre reinforced HDPE composites. Compos Struct. 2018;188:394–406. https://doi.org/10.1016/j.compstruct.2018.01.046.
22. Grubeša IN, Marković B, Gojević A, Brdarić J. Effect of hemp fibers on fire resistance of concrete. Constr Build Mater. 2018;184:473–84.
23. Mostefai N, Hamzaoui R, Guessasma S, Aw A, Nouri H. Microstructure and mechanical performance of modified hemp fibre and Shiv mortars: discovering the optimal formulation. Mater Des. 2015;84:359–71. https://doi.org/10.1016/j.matdes.2015.06.102.
24. Çomak B, Bideci A, Salli Bideci Ö. Effects of hemp fibers on characteristics of cement based mortar. Constr Build Mater. 2018;169:794–9. https://doi.org/10.1016/j.conbuildmat.2018.03.029.
25. Hamzaoui R, Guessasma S, Abahri K, Bouchenafa O. Formulation of modified cement mortars using optimal combination of fly ashes, shiv, and hemp fibers. J Mater Civ Eng. 2020;32:04019354.

26. Ruano G, Bellomo F, Lopez G, Bertuzzi A, Nallim L, Oller S. Mechanical behaviour of cementitious composites reinforced with Bagasse and hemp fibers. Constr Build Mater. 2020;240:117856.
27. Hamzaoui R, Guessasma S, Mecheri B, Eshtiaghi AM, Bennabi A. Microstructure and mechanical performance of modified mortar using hemp fibres and carbon nanotubes. Mater Des 1980–2015. 2014;56:60–8.
28. Yaras A, Ustaoglu A, Gencel O, Sarı A, Hekimoğlu G, Sutcu M, Erdogmus E, Kaplan G, Bayraktar OY. Characteristics, energy saving and carbon emission reduction potential of gypsum wallboard containing phase change material. J Energy Storage. 2022;55:105685.
29. Turan MT. Farklı lif çeşitlerinin ve sodyum silikat solüsyonunun alçı malzeme özelliklerine etkisi, Master's Thesis, Fen Bilimleri Enstitüsü. 2019.
30. Kaplan G, Bayraktar OY, Bayrak B, Celebi O, Bodur B, Oz A, Aydin AC. Physico-mechanical, thermal insulation and resistance characteristics of diatomite and attapulgite based geopolymer foam concrete: effect of different curing regimes. Constr Build Mater. 2023;373:130850.
31. Cho S, Kruger J, van Rooyen A, van Zijl G. Rheology and application of buoyant foam concrete for digital fabrication. Compos Part B Eng. 2021;215:108800.
32. Kursuncu B, Gencel O, Bayraktar OY, Shi J, Nematzadeh M, Kaplan G. Optimization of foam concrete characteristics using response surface methodology and artificial neural networks. Constr Build Mater. 2022;337:127575.
33. Gencel O, Nodehi M, Bayraktar OY, Kaplan G, Benli A, Gholampour A, Ozbakkaloglu T. Basalt fiber-reinforced foam concrete containing silica fume: an experimental study. Constr Build Mater. 2022;326:126861.
34. Naciri K, Aalil I, Chaaba A. Eco-friendly gypsum-lime mortar with the incorporation of recycled waste brick. Constr Build Mater. 2022;325:126770.
35. Gencel O, Bayraktar O, Kaplan G, Benli A, Martínez-Barrera G, Brostow W, Tek M, Bodur B. Characteristics of hemp fibre reinforced foam concretes with fly Ash and Taguchi optimization. Constr Build Mater. 2021;294:123607. https://doi.org/10.1016/j.conbuildmat.2021.123607.
36. Babu KS, Ratnam C. Mechanical and thermophysical behavior of hemp fiber reinforced gypsum composites. Mater Today Proc. 2021;44:2245–9.
37. Kaplan G, Bayraktar OY. The effect of hemp fiber usage on the mechanical and physical properties of cement based mortars. Res Eng Struct Mater. 2021;7:245–58.
38. Bayraktar OY, Kaplan G, Shi J, Benli A, Bodur B, Turkoglu M. The effect of steel fiber aspect-ratio and content on the fresh, flexural, and mechanical performance of concrete made with recycled fine aggregate. Constr Build Mater. 2023;368:130497.
39. Page J, Khadraoui F, Boutouil M, Gomina M. Multi-physical properties of a structural concrete incorporating short flax fibers. Constr Build Mater. 2017;140:344–53.
40. Boulekbache B, Hamrat M, Chemrouk M, Amziane S. Flowability of fibre-reinforced concrete and its effect on the mechanical properties of the material. Constr Build Mater. 2010;24:1664–71.
41. Mahdi RS. Experimental study effect of using glass fiber on cement mortar. J Babylon Univ Sci. 2014;22:162–81.
42. Jaber HA. Effect of glass wool addition on some properties of cement mortar. Eng Tech J. 2016;34.
43. Ganesan K, Rajagopal K, Thangavel K. Rice husk Ash blended cement: assessment of optimal level of replacement for strength and permeability properties of concrete. Constr Build Mater. 2008;22:1675–83.
44. Bayraktar OY, Yarar G, Benli A, Kaplan G, Gencel O, Sutcu M, Kozłowski M, Kadela M. Basalt fiber reinforced foam concrete with marble waste and calcium aluminate cement. Struct Concr. 2023;24:1152–78. https://doi.org/10.1002/suco.202200142.
45. Kunhanandan Nambiar EK, Ramamurthy K. Fresh state characteristics of foam concrete. J Mater Civ Eng. 2008;20:111–7.
46. Naik TR, Malhotra VM, Popovics JS. The ultrasonic pulse velocity method. In: Handb Nondestruct Test Concr. Second ed. CRC; 2003. pp. 8–1.
47. Yurt Ü, Çelikten S, Atabey İİ. Post-fire residual mechanical and microstructural properties of waste basalt and glass powder-based geopolymer mortars. J Build Eng. 2024;94:109941. https://doi.org/10.1016/j.jobe.2024.109941.
48. Çelikten S, Atabey İİ, Bayer Z, Öztürk. Cleaner environment approach by the utilization of ceramic sanitaryware waste in Portland cement mortar at ambient and elevated temperatures. Iran J Sci Technol Trans Civ Eng. 2022;46:4291–301. https://doi.org/10.1007/s40996-022-00955-1.
49. Aygörmez Y, Canpolat O, Al-mashhadani MM, Uysal M. Elevated temperature, freezing-thawing and wetting-drying effects on polypropylene fiber reinforced Metakaolin based geopolymer composites. Constr Build Mater. 2020;235:117502.
50. Gencel O, Benli A, Bayraktar OY, Kaplan G, Sutcu M, Elabade WAT. Effect of waste marble powder and rice husk Ash on the microstructural, physico-mechanical and transport properties of foam concretes exposed to high temperatures and freeze–thaw cycles. Constr Build Mater. 2021;291:123374. https://doi.org/10.1016/j.conbuildmat.2021.123374.
51. Mendes A, Sanjayan JG, Gates WP, Collins F. The influence of water absorption and porosity on the deterioration of cement paste and concrete exposed to elevated temperatures, as in a fire event. Cem Concr Compos. 2012;34:1067–74.
52. Capasso I, Pappalardo L, Romano RA, Iucolano F. Foamed gypsum for multipurpose applications in Building. Constr Build Mater. 2021;307:124948.
53. Asadi I, Shafigh P, Hassan ZFBA, Mahyuddin NB. Thermal conductivity of concrete–A review. J Build Eng. 2018;20:81–93.
54. Verdolotti L, Iucolano F, Capasso I, Lavorgna M, Iannace S, Liguori B. Recycling and recovery of PE-PP-PET-based fiber polymeric wastes as aggregate replacement in lightweight mortar: evaluation of environmental friendly application. Environ Prog Sustain Energy. 2014;33:1445–51.

Publisher's Note